

## Orientation of the Retroreflectors on the GBT Primary Surface

FRED SCHWAB  
May 19, 1991

In the metrology system for control of the active surface of the Green Bank Telescope, laser rangefinders attached to the feed-support structure will be used to survey retroreflectors mounted on the primary-surface actuator assemblies. If the retroreflectors are of conventional design, then they likely cannot be mounted flush with the surface because then the angles of incidence of the laser beams would be so large that adequate performance could not be achieved. Instead, the retroreflectors will probably need to be tilted with respect to the tangent plane of the surface. Tilted, the retroreflectors would need either to protrude above the surface or to be located below the surface and viewed through holes at the corners of the surface panels. In the latter case, the holes might need to be fairly large. Either choice has undesirable electromagnetic consequences (corruption of the beam pattern and generation of standing-wave patterns). In winter months, protruding retroreflectors would be susceptible to damage from sliding frozen precipitate. The purpose of this memorandum is just to investigate the required angles of tilt.

Figure 1 shows measured curves of reflected power versus laser-beam angle of incidence, for two of the types of retroreflectors that the NRAO has evaluated. One type, whose reflecting surfaces are unsilvered, has a sharp drop-off in reflectivity at incidence angles exceeding  $\sim 25^\circ$  (incidence angle here is defined as the departure from normal, or face-on incidence). The type with silvered reflecting surfaces has a smoother reflectivity curve. For both types the reflectivity drops to near zero at incidence angles of  $50^\circ$ . And, for both, the reflectivity exceeds 50% only for angles within  $\sim 20^\circ$  of normal incidence (i.e., within a cone of  $\sim 40^\circ$  opening angle). Although adequate signal-to-noise might be achieved at significantly larger incidence angles than  $20^\circ$ , David Parker comments that spurious reflections would likely cause degraded performance in this regime. He further comments that, in standard engineering practice, systems generally are designed to utilize only these relatively smaller departures from normal incidence.

Figure 2 shows the geometry of the ranging setup for surface metrology, as currently conceived. The laser rangefinders are located at positions  $P_1$ ,  $P_2$ , and  $P_3$  on the feed-support structure.<sup>1</sup>  $P(x, y) = \left(x, y, \frac{x^2 + y^2}{4f}\right)$  is a point on the surface of the dish, a paraboloid of focal length  $f = 60$  meters. The angle  $\theta_i$ , for  $i = 1, 2, \text{ or } 3$ , is the angle between the local surface normal and the line segment  $\overline{PP_i}$  (i.e.,  $\theta_i$  is the departure from normal incidence upon the retroreflector of the  $i$ th laser beam, assuming the retroreflector to be mounted flush with the surface). The intersection of the surface normal with the axis of revolution of the paraboloid (the  $z$ -axis) is also illustrated. The  $z$ -intercept of the surface normal is at a height of  $2f + (x^2 + y^2)/4f$  meters, and the distance from  $P$  to the  $z$ -axis, measured along the surface normal, is  $\sqrt{x^2 + y^2 + 4f^2}$  meters.

Plots of the angles of incidence,  $\theta_1(x, y)$ ,  $\theta_2(x, y)$ , and  $\theta_3(x, y)$ , at arbitrary points  $P(x, y)$  over the entire dish are shown in Figure 3. Obviously, without tilting the retroreflectors the laser-beam angles of incidence over almost all of the dish are unacceptably large for either of the retroreflector types of Figure 1.

<sup>1</sup>Our tentatively chosen locations for the rangefinders are  $P_1 = (-8.4, 0, 60.2)$  meters and  $P_2, P_3 = (0.9, \pm 5.7, 25.8)$  meters. Probably at least four rangefinders will be used for surface metrology, but the laser beams from additional ones will likely lie in between the beams shown in the figure.

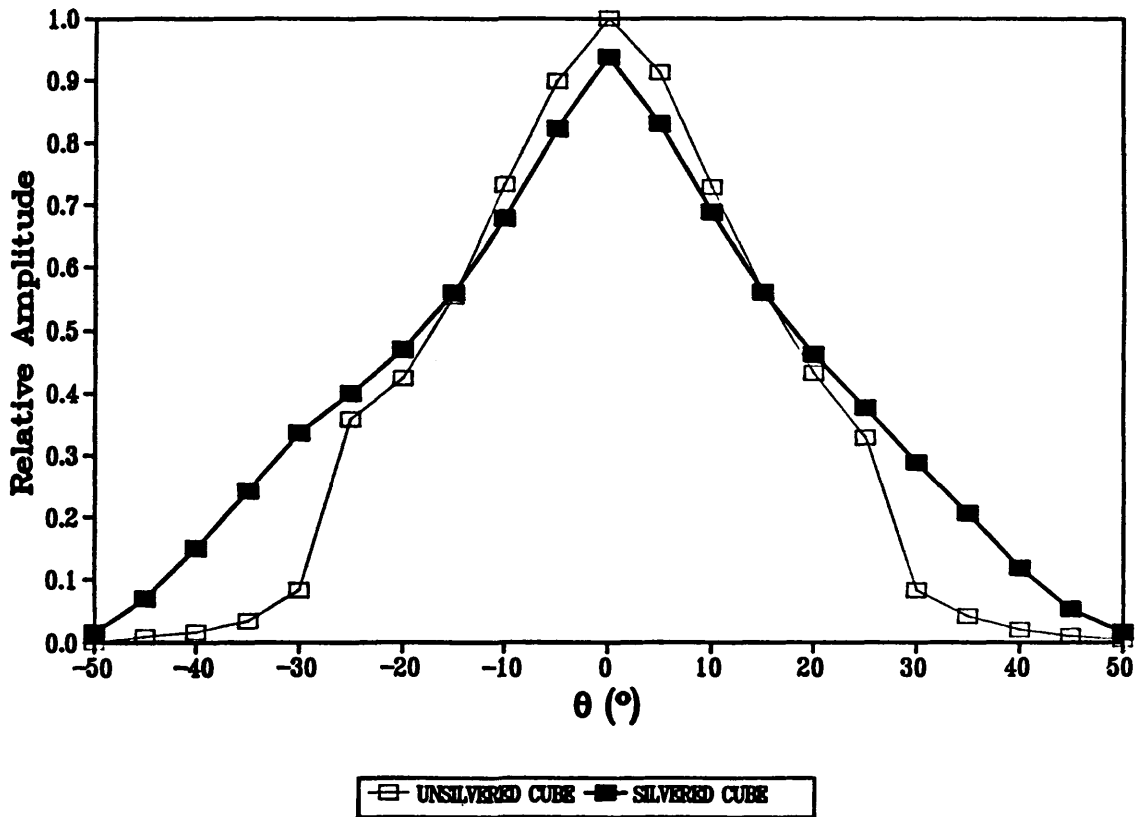


Figure 1. This figure, courtesy of David Parker, shows measured curves of reflected power versus laser-beam angle of incidence, for two of the types of retroreflectors that the NRAO has evaluated. The darker colored curve, with the smoother behavior, is for a retroreflector with silvered reflecting surfaces.

If the retroreflectors are to be tilted, it certainly is best, from a practical standpoint, if the only tilts permitted are tilts about the surface parallels. Permitting no components of tilt about the meridional axes minimizes the required number of different mounting mechanisms. (If we define  $\varphi = \arctan \frac{y}{x}$  and  $r = \sqrt{x^2 + y^2}$ , then the curves  $r = \text{constant}$  are the parallels of the surface, and the curves  $\varphi = \text{constant}$  are the meridians.) I have written a Fortran program to compute the optimal angle of tilt, under the above constraint, for all locations on the GBT design paraboloid. The tilts computed by the program are optimal in the sense of minimizing the maximum value of  $\theta_1$ ,  $\theta_2$ , and  $\theta_3$ . A contour plot of the output of the program is shown in Figure 4.

The optimal tilt angles (for our current choice of rangefinder locations) range between  $\sim 6^\circ$  and  $\sim 50^\circ$ . Instead of designing a mounting mechanism with an adjustable angle of tilt, a sounder engineering solution is probably to design a sufficient number of fixed-angle mounts. How many might be required?

Choosing, at each location on the dish, the best tilt angle that is a multiple of  $5^\circ$  would require ten different types of mount. The laser-beam angles of incidence for this scheme are shown in Figure 5. The largest angle of incidence is  $17^\circ 0'$ .

Figure 6 shows angles of incidence for tilt angles spaced at ten-degree increments, with possible choices  $5^\circ$ ,  $15^\circ$ ,  $25^\circ$ ,  $35^\circ$ , and  $45^\circ$ , requiring five types of mounting mechanisms.

Here, the largest angle of incidence is 18°8.

Finally, Figure 7 shows the situation corresponding to just three types of mounting mechanisms, with tilt angles of 25°, 35°, and 45°. Here the maximum angle of incidence is 23°5. Over almost all of the dish, however, the incidence angles do not exceed twenty degrees. Figure 8 shows the three zones; note that the boundaries between zones are somewhat elliptical, not circular.

It may be possible, with three tilt-angle zones, to improve slightly on the orientation scheme of Figure 7. For example, a scheme with 20°, 30°, and 40° zones has a maximum incidence angle of 19°9. However, the incidence angles at the far edge of the dish then are larger, where the distances to be measured are longer.

### CONCLUSIONS

It seems certain that the retroreflectors will have to be tilted. Three tilts—and thus three types of mounting mechanisms—would appear to be adequate.

### APPENDIX

A tricky part of the calculation in my computer program is to compute a unit vector in the direction defining the desired orientation of the retroreflector. I'll outline that part of the calculation here, since someone on the engineering staff might want to understand my program.

The program needs to know how to rotate a vector about a prescribed axis. The desired axis of the rotation is the direction  $\frac{\partial \mathbf{P}}{\partial \varphi}$ , where  $\mathbf{P}(x, y) = \left(x, y, \frac{x^2 + y^2}{4f}\right) = \left(r \cos \varphi, r \sin \varphi, \frac{r^2}{4f}\right)$  is the position of the retroreflector in space. Differentiating with respect to  $\varphi$ , we get the vector  $(-r \sin \varphi, r \cos \varphi, 0)$ . If, for convenience, we normalize to unit length, we get  $\mathbf{v} = (-\sin \varphi, \cos \varphi, 0)$  as the desired axis of rotation.

Now, to construct the desired rotation matrix, we need two mutually orthogonal unit vectors,  $\mathbf{u}$  and  $\mathbf{w}$ , also orthogonal to  $\mathbf{v}$ . One we may take as a unit vector in the direction  $\frac{\partial \mathbf{P}}{\partial r}$  of the meridian at  $\mathbf{P}(x, y)$ . Thus  $\mathbf{u} = \left(\cos \varphi, \sin \varphi, \frac{r}{2f}\right) / \sqrt{1 + \frac{r^2}{4f^2}}$ . The other then has to be the unit normal at  $\mathbf{P}(x, y)$ :  $\mathbf{w} = (-x, -y, 2f) / \sqrt{r^2 + 4f^2}$ .

Next, we construct a matrix  $\mathbf{Q}$  whose columns are  $\mathbf{u}^t$ ,  $\mathbf{w}^t$ , and  $\mathbf{v}^t$ , in that order.  $\mathbf{Q}$  is an orthogonal matrix; i.e., its transpose is identical to its inverse:  $\mathbf{Q}^t = \mathbf{Q}^{-1}$ . Finally, multiplication of the x-y-z coordinates of an arbitrary vector by the matrix

$$\mathbf{R} = \mathbf{Q} \begin{pmatrix} \cos \psi & -\sin \psi & 0 \\ \sin \psi & \cos \psi & 0 \\ 0 & 0 & 1 \end{pmatrix} \mathbf{Q}^t$$

will rotate the vector by an angle  $\psi$  about the  $\mathbf{v}$ -axis. (Multiplication by  $\mathbf{Q}^t$  transforms to coordinates in the  $\mathbf{u}$ - $\mathbf{w}$ - $\mathbf{v}$  system; the multiplication by the middle matrix accomplishes the rotation about the  $\mathbf{v}$ -axis; and the final multiplication by  $\mathbf{Q}$  transforms back to coordinates in the x-y-z system.) For a reference, see any linear algebra text or see J. D. Talman, *Special Functions*, (Benjamin, 1968), ch. 9, from which I borrowed the notation.

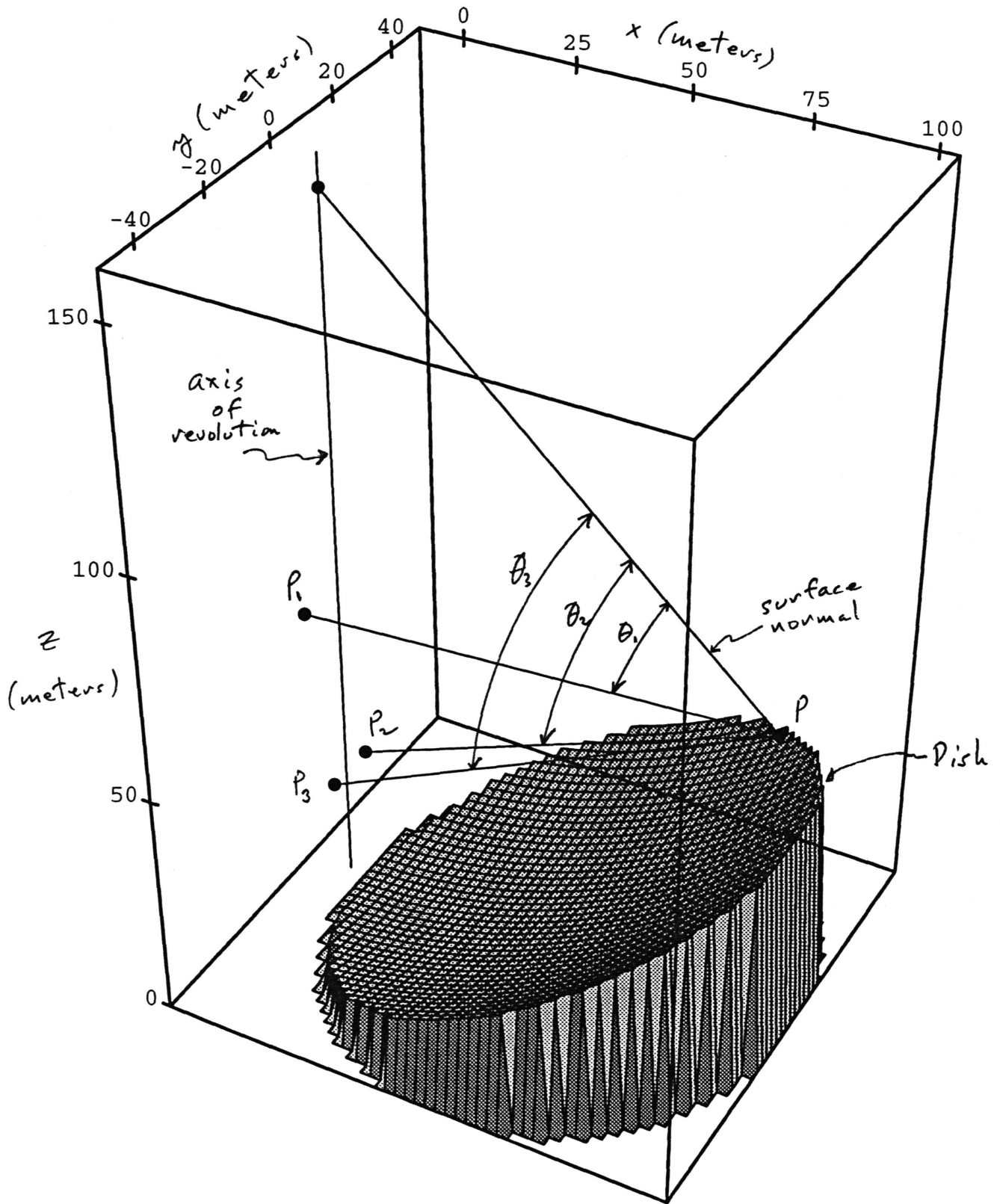


**Figure 2.** Geometry of the rangefinding setup for surface metrology. Rangefinders are located at positions  $P_1$ ,  $P_2$ , and  $P_3$ .  $P$  is a point on the surface of the dish.  $\theta_i$ , for  $i = 1, 2$ , and  $3$ , is the angle between the local surface normal and the line segment  $\overline{PP_i}$  (i.e., the departure from normal incidence upon the retroreflector of the  $i$ th laser beam, assuming the retroreflector to be mounted flush with the surface). The intersection of the surface normal with the axis of revolution of the paraboloid (the  $z$ -axis) is also illustrated.

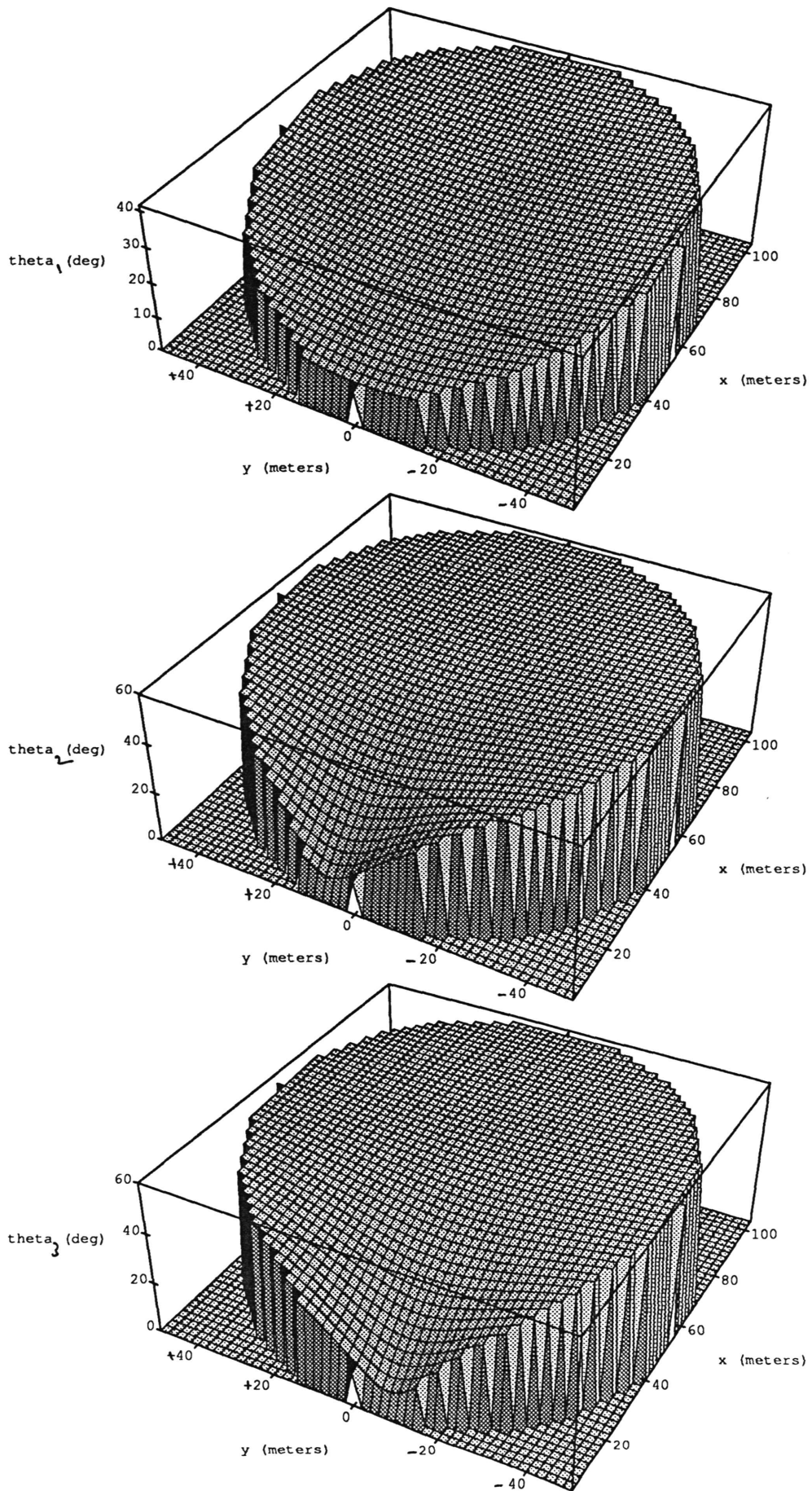


**Figure 3.** Plots of  $\theta_1(x, y)$ ,  $\theta_2(x, y)$ , and  $\theta_3(x, y)$ —the laser-beam angles of incidence if the retroreflectors are mounted flush with the surface—at arbitrary points  $P(x, y)$  over the entire dish.

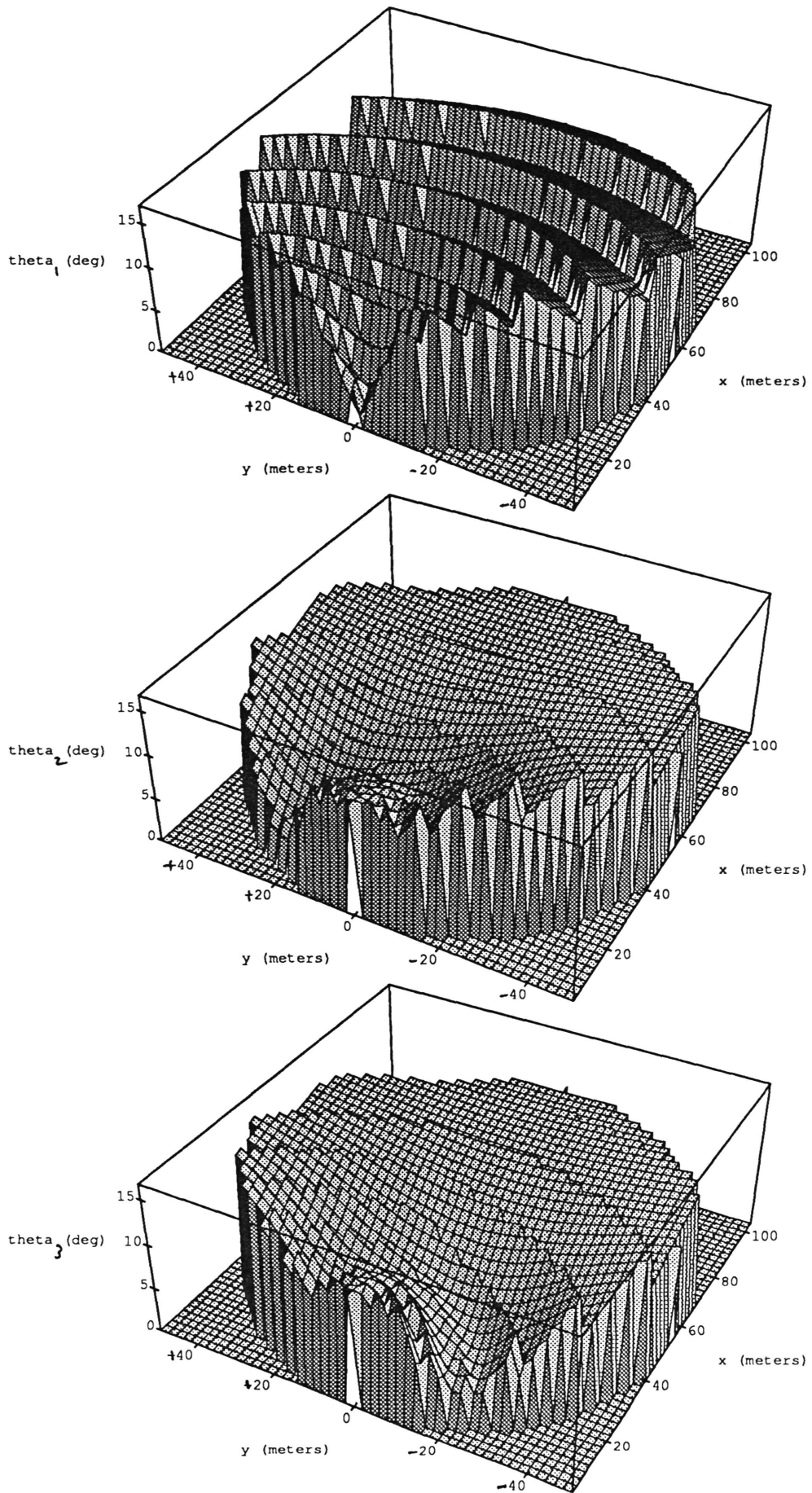


**Figure 5.** Plots of the three angles of incidence,  $\theta_1$ ,  $\theta_2$ , and  $\theta_3$ , for retroreflectors oriented at the optimal angle of tilt among possible choices of  $5^\circ$ ,  $10^\circ$ ,  $15^\circ$ ,  $20^\circ$ ,  $25^\circ$ ,  $30^\circ$ ,  $35^\circ$ ,  $40^\circ$ ,  $45^\circ$ , and  $50^\circ$ .

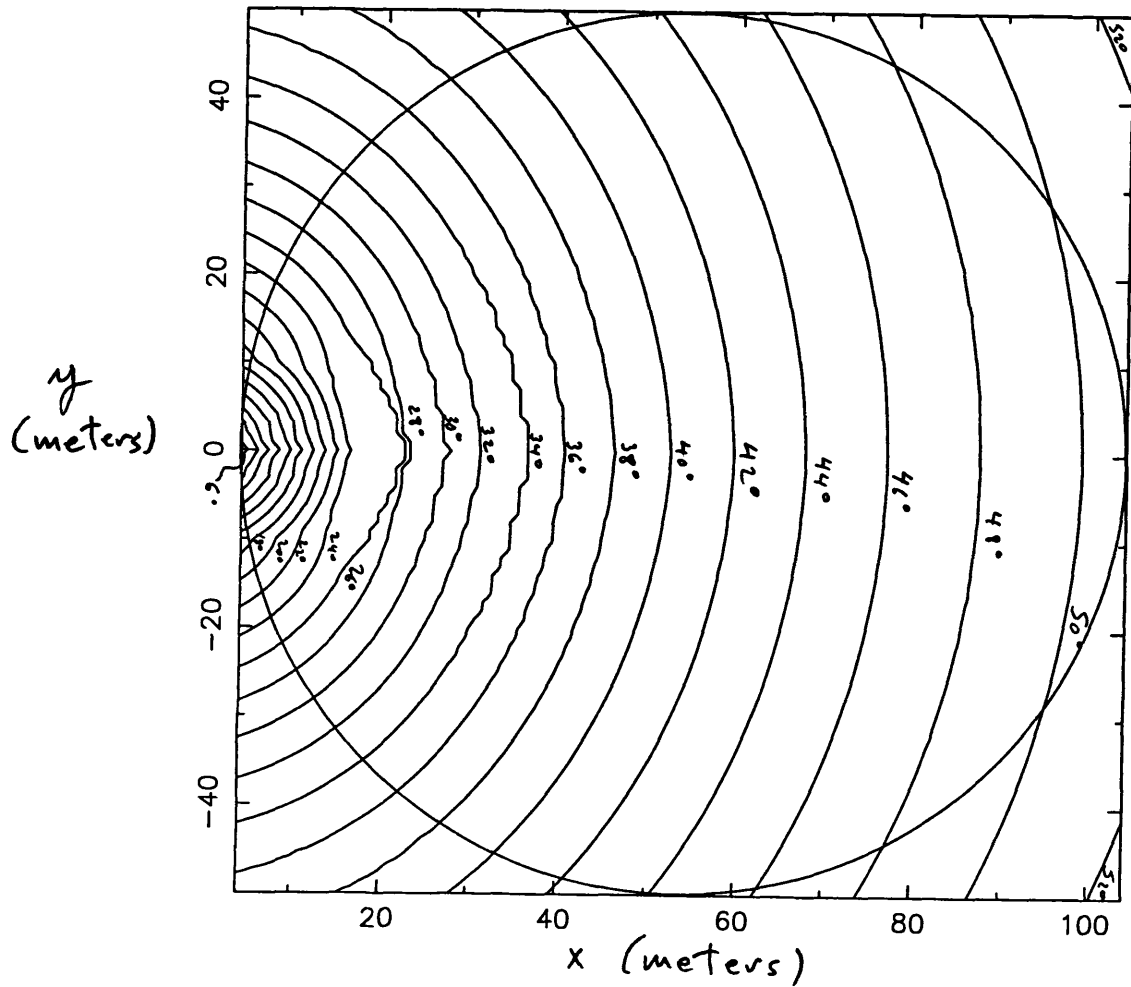


**Figure 4.** A contour plot of the optimal angle of tilt at each location on the dish. The tilt axes are constrained to coincide with the surface parallels. The lowest contour level is  $6^\circ$ , the highest is  $52^\circ$ , and the contour interval is  $2^\circ$ . The function that is displayed has discontinuous derivatives, which accounts for the ragged appearance of the innermost contours.

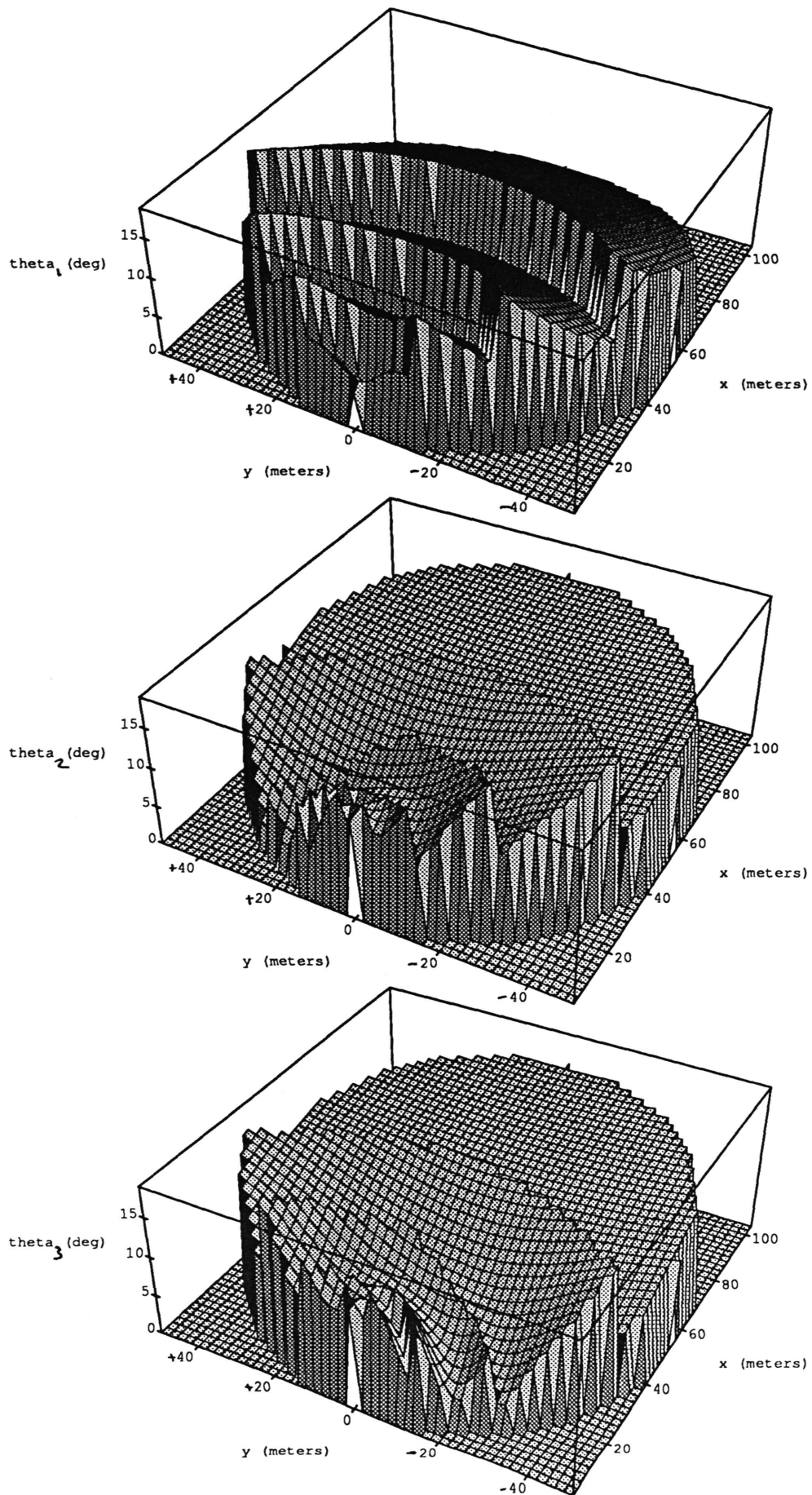


**Figure 6.** Plots of the three angles of incidence,  $\theta_1$ ,  $\theta_2$ , and  $\theta_3$ , for retroreflectors oriented at the optimal angle of tilt among possible choices of 5°, 15°, 25°, 35°, and 45°.

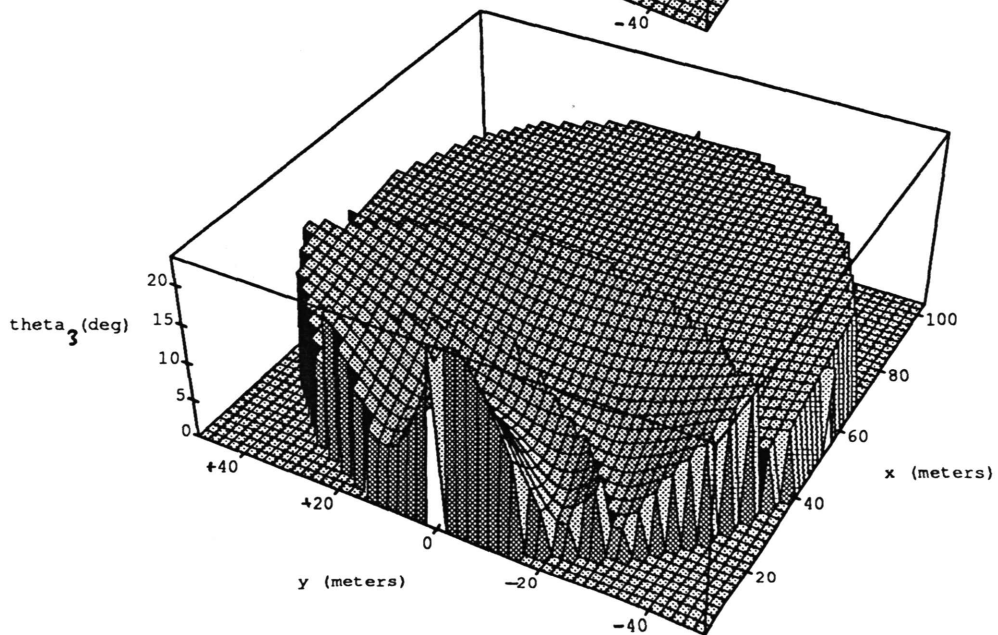
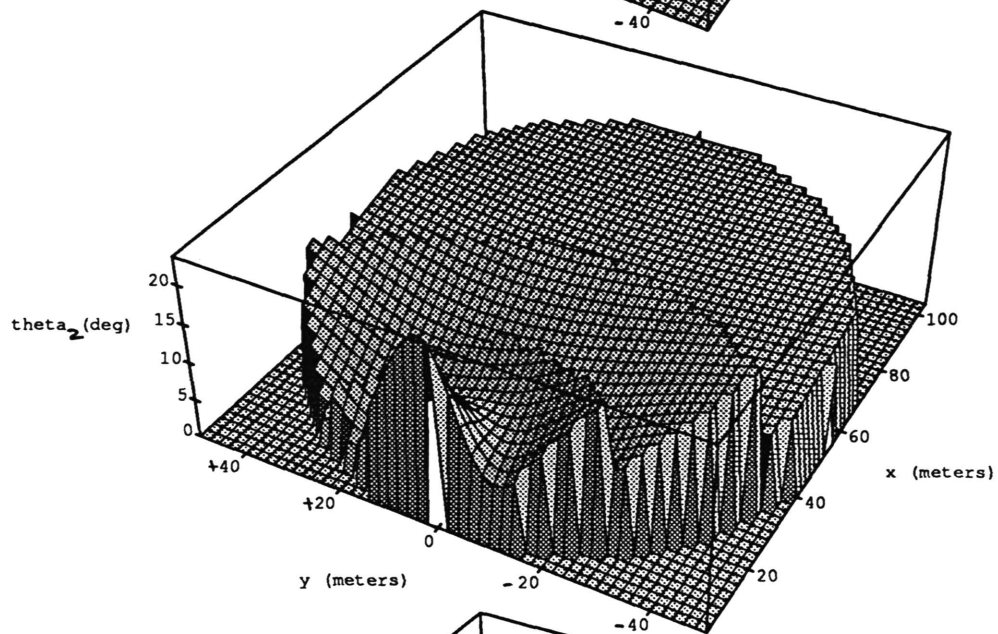
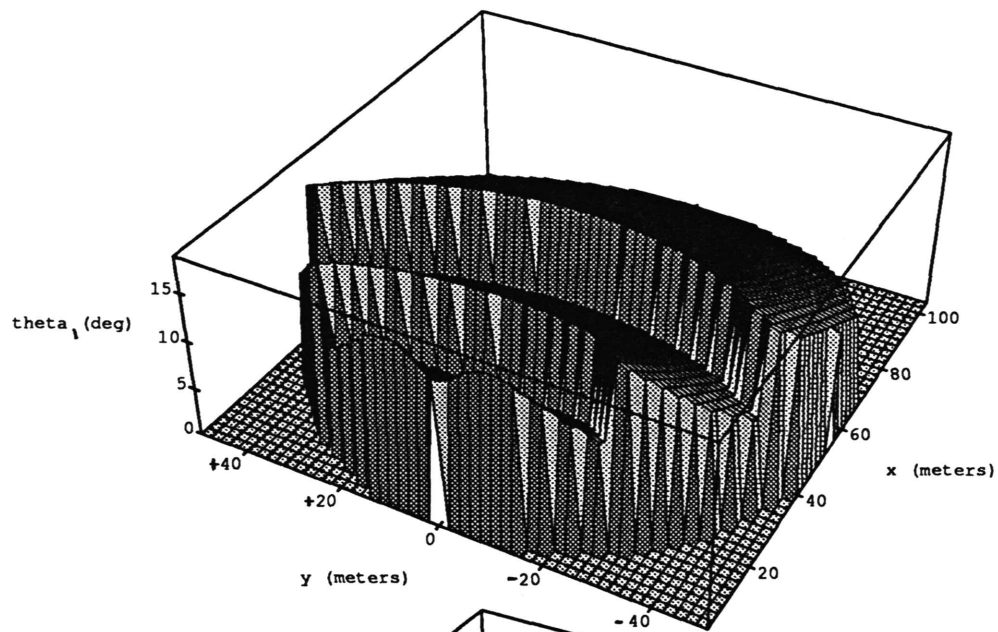


**Figure 7.** Plots of the three angles of incidence,  $\theta_1$ ,  $\theta_2$ , and  $\theta_3$ , for retroreflectors oriented at the optimal angle of tilt among possible choices of  $25^\circ$ ,  $35^\circ$ , and  $45^\circ$ —requiring only three types of mount.

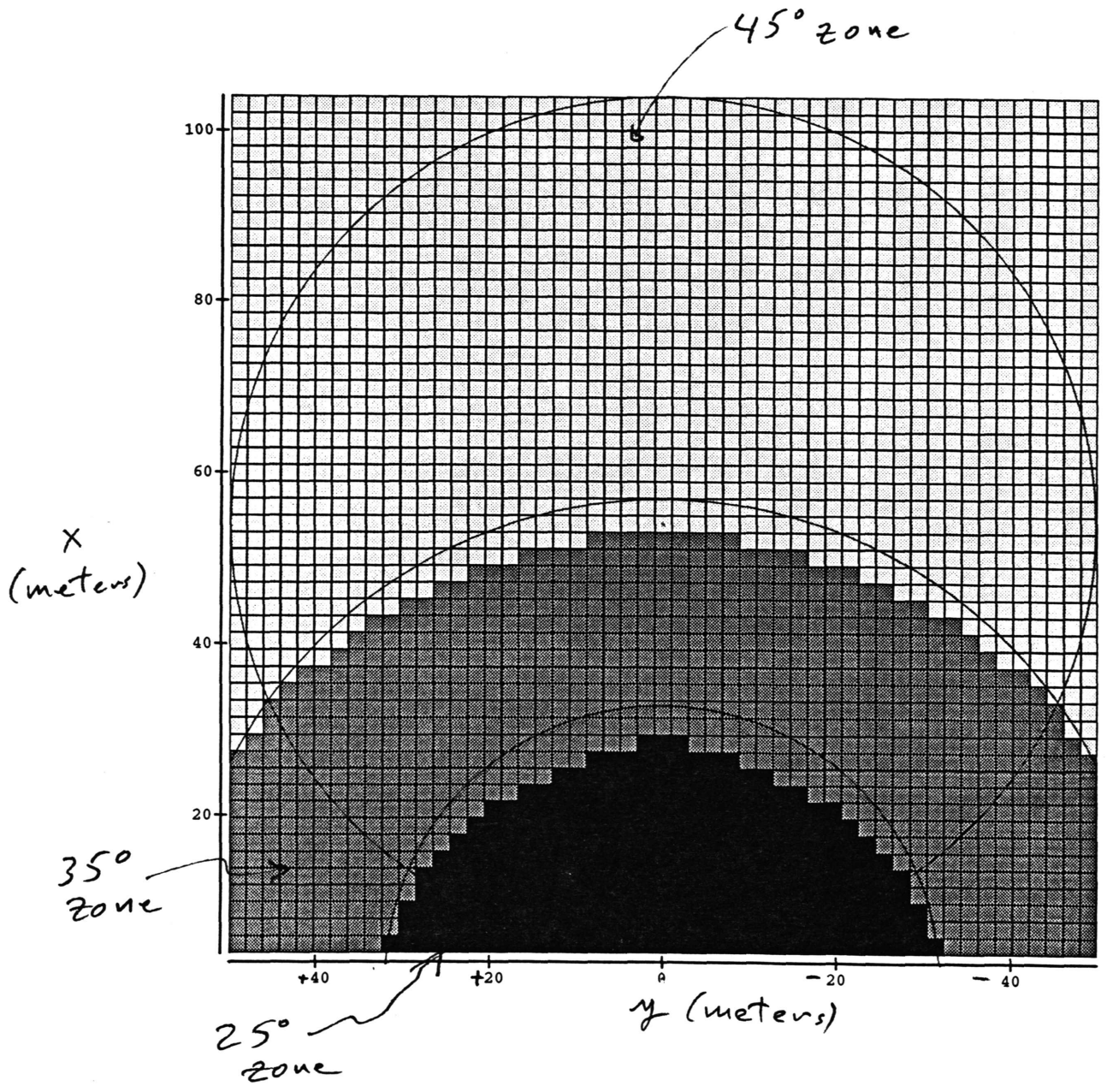


Figure 8. The three tilt-angle zones corresponding to Figure 7.